Environmental Pollution 343 (2024) 123226

Contents lists available at ScienceDirect

Environmental Pollution

journal homepage: www.elsevier.com/locate/envpol

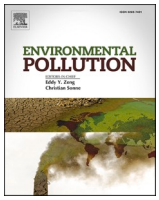

UV light assisted degradation of acid orange azo dye by ZVI-ZnS and effluent toxicity effects☆

Alice Cardito [a], Maurizio Carotenuto [a,*], Olga Sacco [a], Luisa Albarano [b], Vincenzo Vaiano [c], Patrizia Iannece [a], Giovanni Libralato [b], Vincenzo Romano Spica [d], Giusy Lofrano [d]

[a] Department of Chemistry and Biology "A. Zambelli", University of Salerno, via Giovanni Paolo II 132, 84084, Fisciano, SA, Italy
[b] Department of Biology, University of Naples Federico II, via Cinthia ed. 7, 80126, Naples, Italy
[c] Department of Industrial Engineering, University of Salerno, via Giovanni Paolo II, 132, 84084, Fisciano, SA, Italy
[d] Department of Movement, Human and Health Sciences, University of Rome "Foro Italico", 00135, Rome, Italy

ARTICLE INFO

Keywords:
Zero-valent iron
ZnS
Acid orange 7
UV light
Biochar
Toxicity

ABSTRACT

Azo dyes, the most common synthetic dyes used in the textile industry, are known xenobiotic compounds and recalcitrant to conventional degradation treatments. As consequence, such contaminants are often discharged into the effluents, treating aquatic ecosystems. Among several processes, the use of zero valent iron (ZVI) represents a suitable alternative to degrade organic molecules containing azo bonds. However, its applications are limited by corrosion and loss of reactivity over the time. To overcome these constraints, ZVI has been coupled to a suitable semiconductor (ZnS) to get a catalytic composite (ZVI-ZnS) active under UV light. The present work deals with the degradation of acid orange (AO7), used as model azo dye, by UV/ZVI-ZnS, as one step treatment and in combination with an adsorption process by biochar. The influence of ZVI-ZnS concentration (0.25, 0.5, 1 and 2 g/L) and reaction time (0–160 min) on degradation of AO7 were investigated. Intermediates formation was monitored by ESI-FT-ICR-MS analysis and the effluent toxicity was assessed by using *Artemia franciscana*. The experimental results showed that the UV/ZVI-ZnS process at 1 g/L of catalyst allowed to achieve a removal of AO7 up to 97% after 10 min. An increase of the dye relative concentrations as well as the toxicity related to intermediates formations has been observed for treatment time higher than 10 min. The total removal of AO7 together with effluent toxicity reduction was obtained only after the combined treatment (UV/ZVI-ZnS + biochar).

1. Introduction

Synthetic dyes, widely used in many industrial fields such as textile, paper and plastic, have raised environmental concerns because of their contamination of water and soil, their toxicity and poor degradability (Zhang et al., 2012; El-Nemr et al., 2020). It has been estimated that over 700,000 tons of dyestuff are produced annually, and about half of them are azo dyes (Bauer et al., 2001; Freyria et al., 2017; Perera, 2019). Azo dyes are characterized by the presence of one of more azo bonds (–N═N–), generally linked to complex aromatic structures; these dyes constitute a significant burden on the environment, since they can affect the photosynthetic activity of aquatic plants by reducing light penetration, and their breakdown products are usually toxic (Bandara et al., 1999; Cao et al., 1999; Rauf et al., 2011; Satapanajaru et al., 2011; Zhang et al., 2012; Perera, 2019; Zhu et al., 2019). Some azo dyes can break down into aromatic amines, which are known to be dangerous, since can inhibit the biomass growth and cause mutagenicity, carcinogenicity, and other possible biotoxicities effects (Zhang et al., 2004; Lichtfouse et al., 2015; Perera, 2019).

About 15% of the total azo dyes produced worldwide (about 150 tons per day) are released without proper treatment in effluents during manufactory or processing operations, and due to their complex aromatic structures they are resistant to microorganisms and recalcitrant to conventional wastewater treatment based on biological processes (Banat et al., 1996; Bandara et al., 1999; Bauer et al., 2001; Zhang et al., 2012).

Acid Orange 7 (p-(2-hydroxy-1-napthhylazo) benzene sulfonic acid, AO7) is among the most used azo dye and can be considered as a model molecule of the category. It is inexpensive, water soluble, and possesses

☆ This paper has been recommended for acceptance by Dr Amit Bhatnagar.

* Corresponding author.
E-mail address: mcarotenuto@unisa.it (M. Carotenuto).

https://doi.org/10.1016/j.envpol.2023.123226
Received 26 September 2023; Received in revised form 30 November 2023; Accepted 23 December 2023
Available online 28 December 2023

thermal, physical and chemical stability, so it is used for dyeing a variety of materials (wool, silk, nylon, etc.) (Roy et al., 2003; Perera, 2019). Its concentration detected in the final clarifier of a textile factory in India was 45 mg/L (Sivakumar, 2014). According to the literature the dye concentrations discharged from dye houses ranged from 10 to 5000 mg/L (Yaseen and Scholz, 2019). As much now as ever, industries using chemical compounds which are potential contaminants of emerging concern or bio-recalcitrant to conventional treatments, are under enormous pressure from the public and convention rules to adequate the wastewater treatments in order to promote effluents reuse or discharge harmless streams into the ecosystem. Therefore, to find efficient treatment options of such kind of contaminants is becoming essential to make sustainable several industrial processes.

Several methods were proposed in the literature for the removal of AO7, including various advanced oxidation processes (AOPs) such as photocatalysis (Guan et al., 2021), peracetic acid-based processes, adsorption (Xiong et al., 2022; Perez-Calderon et al., 2023) and combined treatments (Sonwani et al., 2021). The adsorption process is the phenomenon that occurs when a molecule or ions present in a fluid (liquid or gaseous) remain on a solid surface, due to the presence of attractive forces between the adsorbent's surface and the adsorbate (Rathi and Kumar, 2021). An efficient absorption of AO7 by activated carbon (AC) or zeolites (Lim et al., 2013) has been reported. More recently, the use of biochar has been also proven as a good method for AO7 removal (El-Nemr et al., 2020). It has been proved a suitable additive for promoting AO7 anaerobic digestion (Zhao et al., 2021) and an activator of peroxydisulfate for AO7 degradation (Zhu et al., 2019). It has been also reported that zero valent iron (ZVI) is an effective reducing reagent used for the treatment of several water pollutants, and its capability of degrading AO7 molecules has been widely proved (Cao et al., 1999; Nam and Tratnyek, 2000; Roy et al., 2003; Mielczarski et al., 2005; Freyria et al., 2011; Zhang et al., 2012; Freyria et al., 2017). The cleavage of the azo bond due to electron donation by ZVI causes the decolorization (Rauf et al., 2011; Satapanajaru et al., 2011). However, corrosion and loss of reactivity over time strongly reduce the practical use of ZVI in remediation processes (Sacco et al., 2021). To overcome these limits, recently ZVI has been paired with a suitable semiconductor constituted by zinc sulfide (ZnS), with high positive redox potential: when irradiated with UV light, ZnS provides electrons to reduce Fe^{2+} back to Fe^0, limiting the ZVI corrosion phenomena (Sacco et al., 2021). Previous studies showed the efficiency of the composite obtained by coupling zinc sulfide (ZnS) semiconductor to ZVI, to degrade chlorinated organic compounds (Sacco et al., 2021). ZVI-ZnS showed a better photocatalytic activity than single catalysts, evidencing that the simultaneous presence of UV light and ZnS avoid the Fe^0 oxidative corrosion phenomena, also assuring its high reactivity after several reuse cycles. Under UV light, the photoexcited electrons in the ZnS conduction band (ECB = −1.04 eV vs. NHE) can effectively reduce Fe^{2+} into Fe^0 (E^0 = −0.44 eV vs. NHE).

Respect to some benefits of the surface adsorption process, including simple design, operation and low initial cost, as well as lower energy source, the zero valent iron/zinc sulfide composite (ZVI-ZnS) under UV lights as one-step treatment (UV/ZVI-ZnS) process potentially allows to achieve a complete degradation of target dye. However, to properly assess the process behaviour, ecotoxicity test should be performed since it is well known that process intermediates or by-products can be more toxic than parent compound.

In this work, the removal of AO7 from water solutions using a UV/ZVI-ZnS and in combination with a biochar unit was investigated. Additionally, ecotoxicity tests were carried out on treated samples, using *Artemia franciscana* as the target species to assess the environmental compatibility of the effluents.

2. Materials and methods

2.1. Materials

Zinc sulfide (ZnS), sodium borohydride ($NaBH_4$) and iron (II) sulfate heptahydrate ($FeSO_4{\cdot}7H_2O$) were purchased by Sigma–Aldrich. AO7 with purity equal to 99.9% was purchased from Romil. Biochar with a high porosity and 70% of carbon content, produced through the gasification of virgin wood was furnished by Reset S.p.A (Rieti, Italy). In Fig. S1 the structural formula of AO7 dye is reported. In aqueous phase, the compound undergoes a very fast intramolecular proton transfer which leads to a tautomerism, so that both the azo form (A) and hydrazone form (B) are simultaneously present. The hydrazone form has usually a higher tinctorial strength (Bauer et al., 2001).

2.2. ZVI-ZnS preparation

The ZVI-ZnS composite was prepared following the procedure reported by Sacco et al. (2021). Specifically, 1.0 g of ZnS semiconductor was dispersed in 100 mL of an aqueous solution of $FeSO_4{\cdot}7H_2O$ (4.0 g). The suspension was stirred for 10 min in presence of He flow (flow rate: 30 NL/h), in order to remove the dissolved oxygen generally present in aqueous phase. Then, $NaBH_4$ (1.4 g), used as reducing agent, was added to the suspension that was kept stirred in the presence of He flow for 1 h. After that, the suspension was centrifuged, washed with distilled water three times, and finally dried overnight at room temperature, obtaining ZVI-ZnS composite. ZVI content in the ZVI-ZnS composite was 45 wt%. The composite was deeply characterized in our previous works (Sacco et al., 2021). In detail, wide-angle X-ray diffraction (WAXD) analysis of ZVI-ZnS evidenced diffraction patterns (at 2θ = 28.6, 33.2, 47.6 and 56.5°) due to ZnS, and the characteristic peak of ZVI, at about $2\theta = 45°$. Temperature-programmed reduction (TPR-H_2) measurements evidenced an interpenetrated structure of the ZVI and ZnS phases as well as the presence of some iron in an oxidized form (Rescigno et al., 2023). Moreover, photoluminescence spectral analysis (PL) showed that the PL signals intensity of ZVI-ZnS was lower than that ZnS alone, evidencing that the presence of ZVI in the composite allows to capture the photoactivated electrons and thus slows down the recombination phenomena between the electrons (promoted in the conduction band of ZnS) and the positive holes (generated in the valence band of ZnS) (Rescigno et al., 2023).

2.3. Experimental procedures

For degradation experiments, 20 mg/L of AO7 solutions were prepared by dissolving the dye in deionized water. In each test, a volume of 100 mL of solution with a given amount of ZVI-ZnS were used. Four different ZVI-ZnS dosages were considered: 0.25, 0.5, 1 and 2 g/L. Suspensions were transferred in a 250 mL beaker, kept on a magnetic stirrer for the duration of the test. Each experiment lasted 160 min, and samples were collected after 0, 1, 2.5, 5, 10, 15, 20, 40, 80, and 160 min. The suspension was irradiated with 2 UV-A lights (TL 8W BLB provided by Philips; with main emission wavelength at 365 nm). After collection, samples were centrifuged (ALC 4236-A Centrifuge), and AO7 residual concentration in the supernatant was monitored through UV–Vis spectroscopy (Cary® 50 UV–Vis Spectrophotometer – Agilent, equipped with a quartz cell, 1 cm optical path), by following the intensity of its characteristic peak at 484 nm (Freyria et al., 2011). A blank experiment was carried out without ZVI-ZnS but in presence of UV-A radiation to evaluate the possible photolysis of AO7.

The biochar unit was constituted by a column filled with 2 g of biochar pruning clippings. The column was fed by a beaker of 250 mL, containing the pre-treated solutions, using a peristaltic pump (Watson Marlow 120U) to recirculate the solution for 55 min at 2 mL/min.

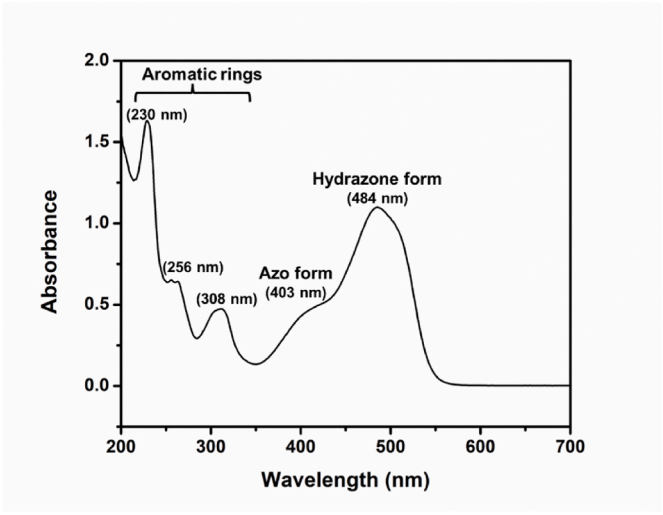

Fig. 1. UV–Vis absorbance spectrum of AO7 solution (20 mg/L).

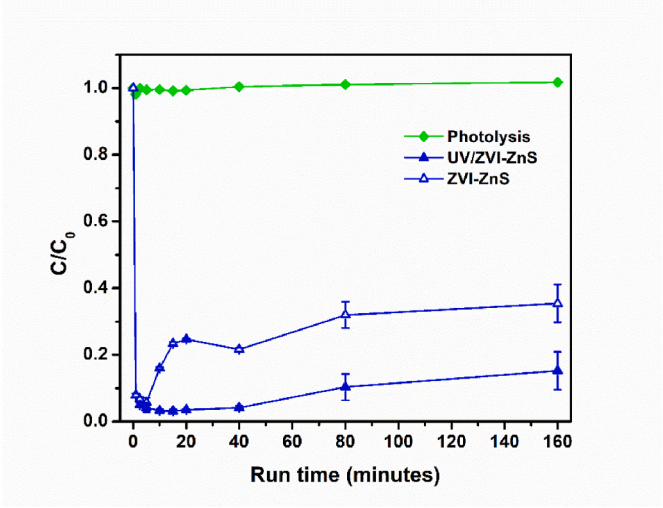

Fig. 2. Trend of AO7 concentration, expressed as C/C0 vs. run time, during photolysis and treatment with 1 g/L of ZVI-ZnS under irradiated and non-irradiated conditions.

2.4. ESI-FT-ICR-MS analysis

High-resolution mass spectra of AO7 solutions and treated effluents were acquired on a SolariX XR 7T FT-ICR-MS equipped with an electrospray ion source ESI (Bruker Daltonik GmbH, Bremen, Germany). Mass spectra were acquired in negative ion mode in a mass range of 50–1000 m/z. The capillary voltage was set to 3.9 kV, with a nebulizer gas pressure of 1.2 bar and dry gas flow rate of 4 L/min at 200 °C. Samples (10 mg/L in CH_3OH) were infused at 4 μL/min, with an ion accumulation of 20 ms, with 16 scans and using 2 million data points (2M). Before the analysis, the mass spectrometer was externally calibrated with NaTFA. High mass accuracies were reached for the NaTFA calibration datasets, with a root mean square (RMS) error lower than 0.2 ppm. MS/MS of the ion of interest was obtained by isolation in the quadrupole and ramping the collision energy manually. The FT-ICR MS mass spectra were processed by using the Bruker DataAnalysis software (v. 4.2).

2.5. Ecotoxicity tests

Ecotoxicity tests were carried out on samples from the experiment with UV/ZVI-ZnS process, collected after 10 or 160 min after the start of the treatments, to monitor the toxicity of the sample. Additionally, an ecotoxicity test was carried out on the solution after the combined UV/ZVI-ZnS + biochar treatment. The target used for ecotoxicity tests was *Artemia franciscana,* a zooplanktonic crustacean commonly known as brine shrimp, considered a suitable organism due to intrinsic characteristic of the genus, such as adaptability to wide ranges of salinity and temperature, short life cycle, high fecundity, small body size, and adaptability to varied nutrient resources (Nunes et al., 2006; Libralato, 2014). The tests were carried out on different states of living: nauplii, metanauplii, juvenile and adult according to standard methods (APAT, IRSA-CNR, 2003) for assessing the lethality. Mortality was measured after 48 h of exposure for all different tested life stages. The experimental procedures for the hatching cysts and incubation of organisms with treatment were carried out according to Albarano et al. (2022a, 2022b). The plates were kept at 25 ± 1 °C with salinity 35 ppm for 48 h in a light regime of 16:8 h/light:dark, without providing food. At 48 h, the number of organisms (which were motionless for 10 s) was counted under a stereomicroscope (Leica EZ4 HD) to calculate the mortality. Tests were considered as significant when mortality in control organisms was <10% after 48 h. All the experiments were performed in triplicates. Toxicity data were reported as mean ± one standard deviation (SD). Data were checked for normality using the Shapiro–Wilk's (S–W) test ($p < 0.05$). The statistical significance of differences among different percentage of treatments and control was checked by two-way ANOVA followed by Tukey's test for multiple comparisons (Prism Software

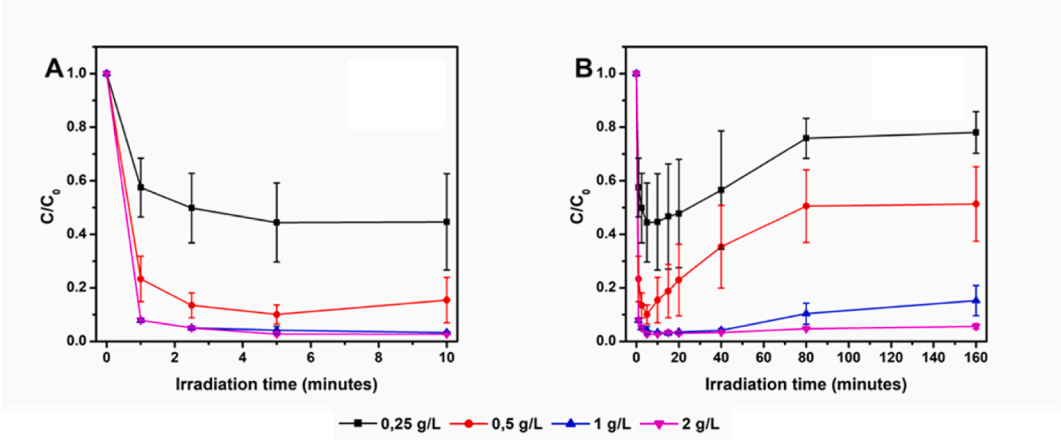

Fig. 3. Effects of dosage concentration of ZVI-ZnS on AO7 concentration, expressed as C/C0 vs. irradiation time (A: 10 min; B: 160 min).

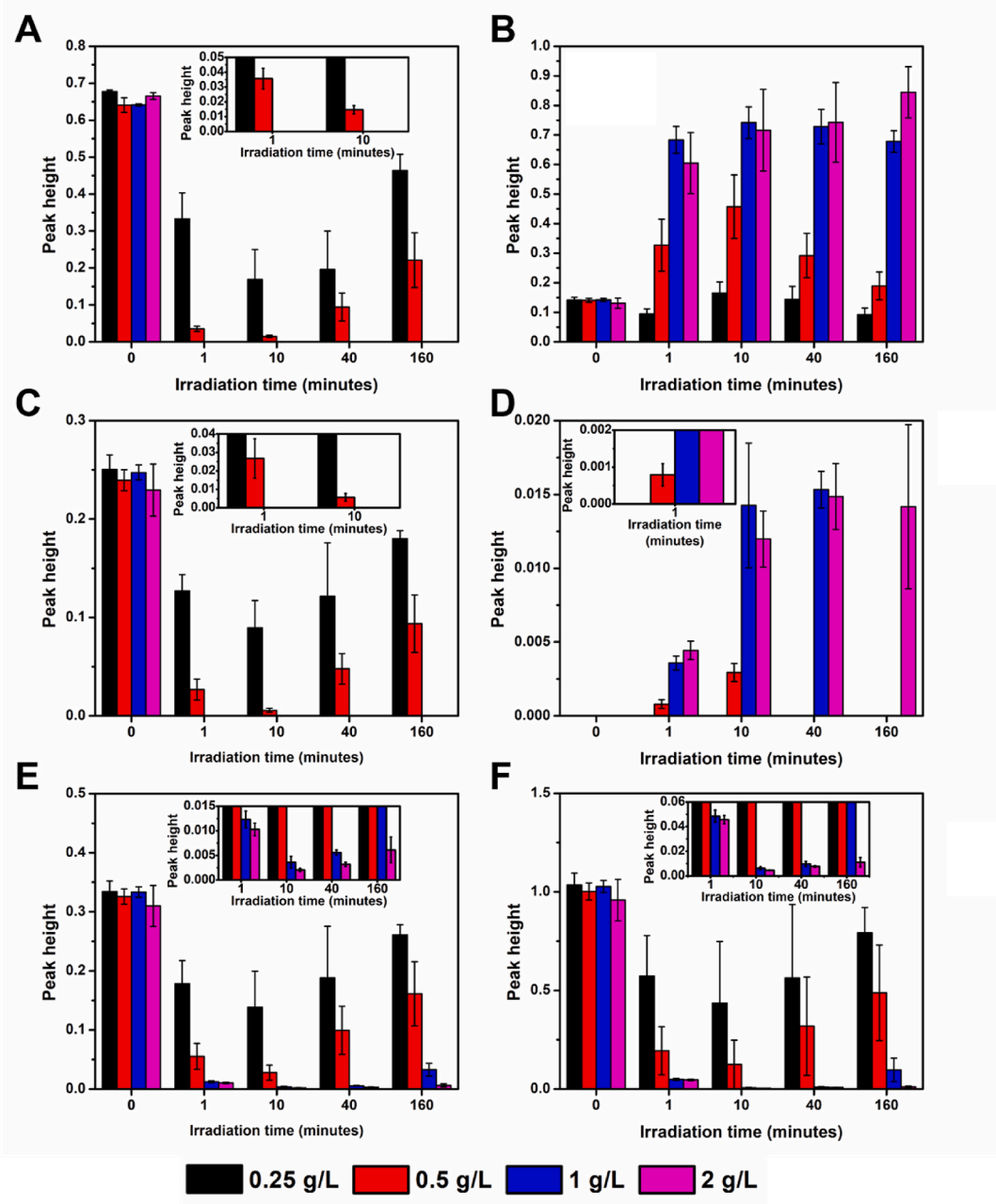

Fig. 4. – Change of absorbance values at 230 nm (A), 250 nm (B), 308 nm (C), 345 nm (D), 403 nm (E) and 484 nm (F) versus time e for different concentrations of ZVI-ZnS under UV-A radiation. When present, the insets show a magnification of the plots.

version 9 for Windows, GraphPad Software – La Jolla, California, USA). p-values < 0.05 were considered statistically significant.

3. Results and discussion

3.1. UV/ZVI-ZnS process and adsorption tests with biochar

The UV–Vis absorbance spectrum of the AO7 solution (20 mg/L) is reported in Fig. 1. The spectrum presents a main band at $\lambda_{max} = 484$ nm, with a shoulder at 403 nm. These two peaks are due the electron transition involving the N–N group of the hydrazone and azo form, respectively (Bauer et al., 2001; Freyria et al., 2011; Freyria et al., 2017). Other bands are observed in the UV region, at 308 nm and 230 nm, that are ascribed to the naphthalene and benzene rings of the dye, respectively (Zhang et al., 2012). The shoulder at 256 nm is also caused by aromatic rings absorption (Freyria et al., 2011; Freyria et al., 2017).

A photolysis experiment was preliminarily carried out by irradiating the AO7 solution with UV-A light. As it is clearly observed in Fig. 2, the concentration of the dye did not change for the whole duration of the test (160 min). Experiments carried out under dark proved a decrease of the degradation performances obtained with ZVI-ZnS when the reaction time increased from 10 to 160 min (Fig. 2). This result was in agreement with literature. The mechanism of AO7 reaction with ZVI proposed by Cao et al. (1999) is reported in Figura 2S. The reaction takes place at the solid-liquid interface and involves the adsorption of the sulfonate group on iron (Roy et al., 2003; Mielczarski et al., 2005; Freyria et al., 2011; Zhang et al., 2012).

A behaviour similar to those observed in dark experiments was registered also during the UV light assisted degradation by ZVI-ZnS treatment (Fig. 2). A rapid discoloration in the first minutes of the reaction was observed, whereas the degradation decreased at longer times.

As shown in Fig. 3 for all concentrations considered, the presence of

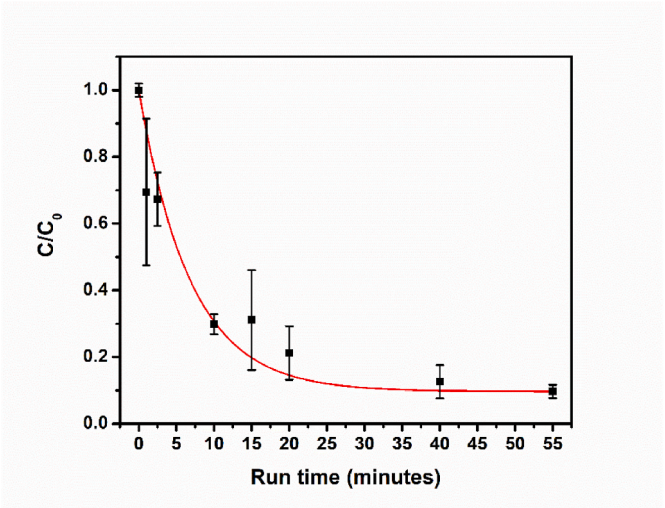

Fig. 5. Removal of residual color (evaluated at 484 nm) during biochar treatment. (For interpretation of the references to color in this figure legend, the reader is referred to the Web version of this article.)

UV light allowed to achieve a more efficient degradation of the dye, respect to dark condition. The enhanced degradation performances observed in presence of UV light is possible due to the high efficiency of ZVI in the reductive cleavage of N═N bond of AO7 and to the ability of electrons promoted in the conduction band of photoexcited ZnS in the reduction of Fe^{2+} (formed by the reductive cleavage of N═N bond to ZVI (Sacco et al., 2021).

Accordingly, as shown in Fig. 3A, the degradation of AO7 improved with the increase of ZVI-ZnS dosage, resulting equal to 55% for 0.25 g/L, 85% for 0.5 g/L, and 97% for both 1 g/L and 2 g/L, after 10 min of treatment in presence of UV light. It is well stated in the literature that up to certain dosage, the increase of catalyst in slurry photocatalytic processes generally strongly influence the degradation of organic compounds (Lofrano et al., 2016). It is worthwhile to note that in the first 10 min of the reaction, the error bars for the test carried out at 0.25 g/L never overlay with the error bars for the test at 0.5 g/L (Fig. 3A). Thus, it is possible to state that the test at 0.5 g/L allowed to achieve a better degradation than the test at 0.25 g/L. At 15, 20 and 40 min some overlays can be observed, however at 80 and 160 min no further overlays appear. Thus, also in this case, we could assume that at the end of the treatment the use of 0.5 g/L is better than 0.25 g/L (Fig. 3B).

The dye relative concentrations increased for treatment time higher than 10 min (Fig. 3B), except for 2 g/L of ZVI-ZnS dosage which allowed a removal of AO7 higher than 97% also after 160 min.

In this first phase of the reaction, the peaks at 484 nm and 403 nm decreased together, indicating that both tautomeric forms react with the same rate or are at mutual equilibrium. Bands at 308 nm and 230 nm also decreased, while the bands at 250 nm and at 345 nm increased, albeit weakly. (Fig. 4). This shows the destruction of the chromophore of the azo dye through the cleavage of the –N═N– bond, and the subsequent formation of the products (substituted aromatic amines) of the reaction, as seen in Fig. S2. These compounds can undergo further transformations: the 4-aminobenzenesulfonate forming sulfanilic acid and the 1-amino-2-naphthol being hydrolyzed to 1,2-dihydroxynaphthalene, and then oxidized to o-naphthoquinone. The two growing band observed during the process can be attributed to these two compounds: the former at 250 nm to sulfanilic acid, while the other at 345 nm to o-naphthoquinone (Fan et al., 2009; Freyria et al., 2011).

When the reaction time increased up to 160 min, the bands at 484 nm, 403 nm, 308 nm and 230 nm grows again while the ones at 345 nm and 250 nm decrease. The overall degradation performance after 80 min was 22% for 0.25 g/L, 49% for 0.5 g/L, 85% for 1 g/L and 94% for 2 g/L

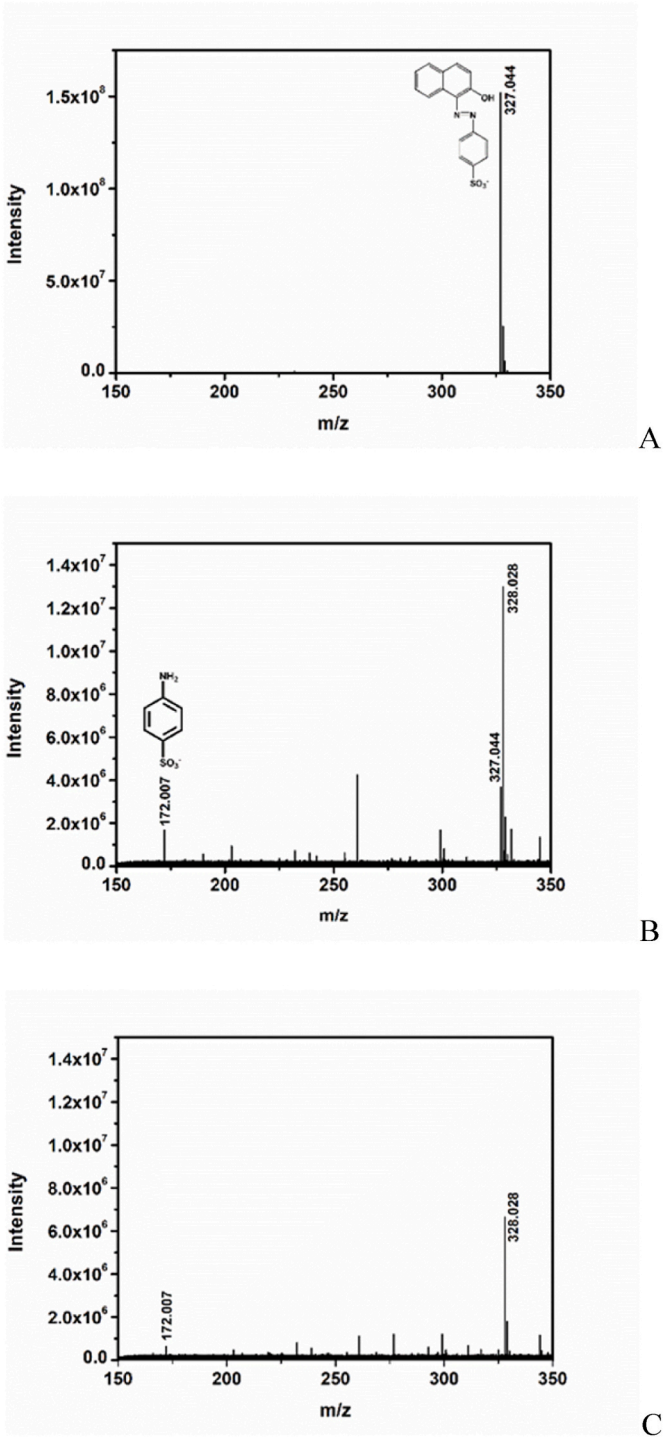

Fig. 6. ESI-MS spectra on (A) untreated AO7(20 mg/L); (B) 1 min of UV/ZVI-ZnS (1 g/L), (C) 160 min of UV/ZVI-ZnS (1 g/L).

and reached a plateau up to 160 min (Fig. 3b).

A similar behavior was observed also by Cao et al. (1999), Freyria et al. (2011) and Freyria et al. (2017), and several explanation were proposed, respectively: (I) the first step of the reaction (Fig. 2S) is reversible, and some of the unstable transitional compound does not decompose in the reaction products but returns to AO7; (II) o-naphthoquinone and the sulfanilic anion reacts together to form an imino compound similar in nature to AO7, responsible for the absorbance at 484 nm; (III) the further oxidation of the surface iron to Fe^{3+} causes the desorption of AO7, since it does not adsorb on fully oxidized surfaces.

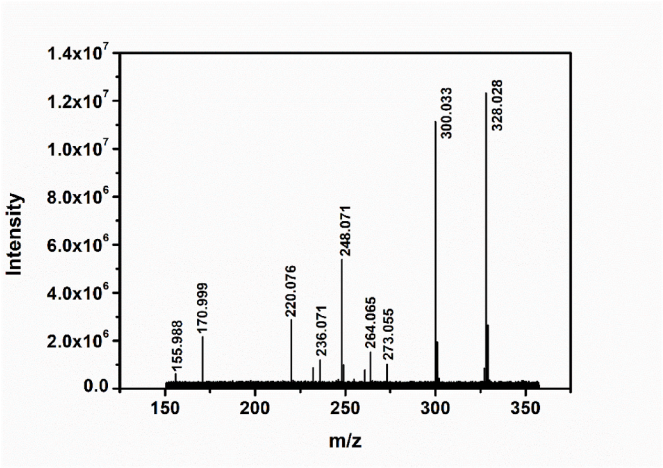

Fig. 7. MS/MS spectrum of 328.028 m/z peak.

For this reason, a combined process was developed by adding an adsorption biochar unit. As shown in Fig. 5, after 55 min of adsorption treatment the removal of residual color (evaluated at 484 nm) from the solution treated with UV/ZVI-ZnS (1 g/L dosage) was equal to about 90%. The adsorption kinetic fits with an exponential curve with rate constant value of 0.14 ± 0.03 1/min ($R^2 = 0.93$).

3.2. Possible reaction intermediates of UV/ZVI-ZnS process

The ESI-MS spectrum on untreated AO7 (20 mg/L) was reported in Fig. 6a, where a peak at 327.044 m/z negative ion is observed. After 1 min of UV/ZVI-ZnS (at 1 g/L dosage), the peak at 327.044 decreased and a peak at 172.007 m/z (negative ion with z = 1) appeared (Fig. 6b), corresponding to 4-aminobenzenesulfonate, according to the mechanism of degradation proposed in the literature (Cao et al., 1999; Zhong et al., 2011). The peak associated to 1-amino-2 naphthol could not be revealed because the negative mode of ESI analysis which does not allow to detect neutral compounds. Moreover, the formation of a compound with a peak at 328.028 m/z negative ion could be registered. After 160 min of UV/ZVI-ZnS (at 1 g/L dosage), the peak at 172.007 m/z (negative ion with z = 1) was still present, whereas the peak at 327.044 was disappeared meaning that the AO7 pristine was completely degraded and the peak at 328.028 m/z negative ion started to decrease (Fig. 6c).

In order to identify the peak at 328.028 a MS/MS analysis was carried out (Fig. 7). The fragmentation of this ion peak using collision induced fragmentation (CID) give important insight into the possible structure of the ionized molecule. In CID experiments, the isolated precursor ions at 328.028 m/z were collisional activated using 20 V. At 20 V, the following fragments: 159.988 m/z; 170.99 m/z; 248.071 m/z were attributed to the molecular structures shown in Table S1. As consequence, it was possible to hypothesize the molecular structure of 328.028 (Table S1). Elemental compositions of all the hypothesized ions were confirmed by Fourier Transform ion cyclotron resonance ESI mass spectrometry (FT-ICR-ESI/MS).

3.3. Ecotoxicity tests

AO7 solution (20 mg/L) caused mortality (about 20–30%) in all life stages already at 6.25% that was statistically significant respecting to control and all other concentrations ($p < 0.0001$; Fig. 8 and Figg. S3–S5; Table S2). The mortality in all life stages at 100% solution involved all organisms. In Figs. 8 and S3-S5, the results of the ecotoxicity tests carried out on samples with different ZVI-ZnS concentrations (0.25 g/L, 0.5 g/L, 1 g/L, 2 g/L) after 160 min of reaction are reported. The treatment

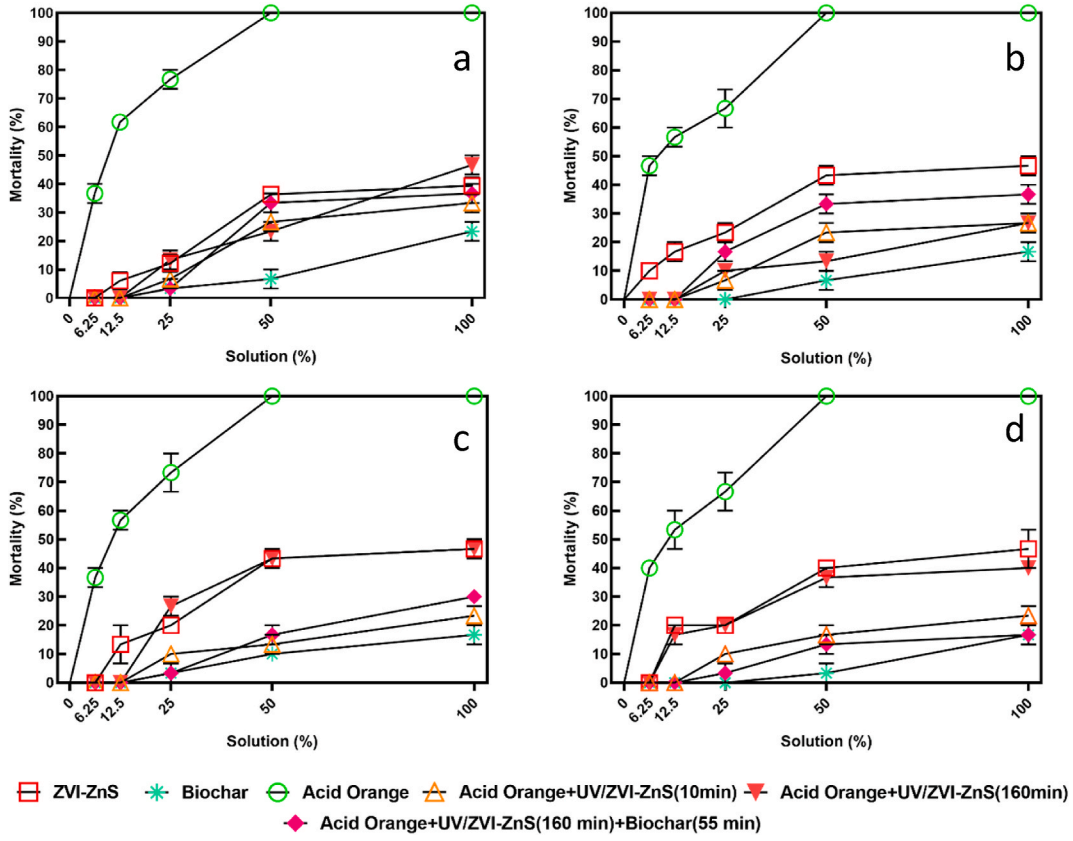

Fig. 8. –Percentage of dead a) nauplii, b) metanauplii, c) juvenile and d) adults detected both in control (0%) and treated samples with 6.25%, 12.5%, 25%, 50%, and 100% of solution. Data are reported as mean ± standard deviation.

greatly reduces the toxicity of the starting AO7 solution for all *Artemia* stages, and in most cases, it could be considered as residual toxicity due to the presence of ZVI-ZnS. Specifically, after 48 h of exposure to different percentage of aqueous solutions of ZVI-ZnS at 0.25 and 0.5 g/L (Figs. S3–S5), an increase of nauplii, metanauplii, juvenile and adult mortality (about 10–20%) was observed only at higher tested percentage, represented by 50% and 100%. These data were statistically significant respecting to the control and others used concentrations ($p < 0.0001$; see also Table S2).

When considered ZVI-ZnS at 1 and 2 g/L, about 20% of toxicity has been shown in all life stages already at 25% of dilution that was statistically significant respecting to control and all other concentrations ($p < 0.0001$; Figs. 8 and S4; Table S2). Since after exposure with treated effluent (Acid Orange + UV/ZVI-ZnS condition) (Fig. 8, S3-S5 and Table S3), we observed similar effects reported in aqueous solutions of ZVI-ZnS, it could be considered residual toxicity due to the residual presence of ZVI-ZnS. Two solutions at higher concentration of catalyst (1 g/L and 2 g/L of ZVI-ZnS) were also analyzed after 10 min from the start of the reaction, that is the moment when AO7 concentration reached its minimum (Figs. 3b, S4). It can be seen that the toxicity after 10 min is lower than the toxicity after 160 min, considering the same concentrations (Fig. 8). Thus, it can be concluded that the toxicity detected after 160 min of treatment was only partially related to due to the residual presence of ZVI-ZnS.

The toxicity test carried out on the treated effluent after 160 min of UV irradiation with ZVI-ZnS at 1 g/L, additionally treated with biochar (2 g/L) for 55 min, showed that the adsorption on biochar additionally lowers the solution toxicity, especially for the juvenile and adult stages (Fig. 8). In fact, about 30–40% of nauplii and metanauplii mortality and less than 20% of juvenile and adult mortality were observed at higher tested percentage (50% and 100%). These data were statistically significant respecting to control and all other concentrations ($p < 0.0001$; Table S3).

4. Conclusions and perspective

The UV/ZVI-ZnS process allowed to achieve a 97% of AO7 degradation after 10 min of treatment. The increase of treatment time determined an overall decrease of degradation performance. However, by adding a biochar unit, a complete removal of AO7 could be achieved. By intermediates analysis through ESI-MS, 4-aminobenzenesulfonate could be identified and the formation of a peak at 328.028 m/z was registered. Molecular structures associated with the peaks previously detected were associated after MS/MS fragmentation. Toxicity studies proved that the adsorption on biochar additionally lowers the solution toxicity, especially for the juvenile and adult stages of *Artemia franciscana*. On the basis of the obtained results, the UV/ZVI-ZnS process followed by an adsorption unit filled with biochar can be recommend as treatment for water polluted by azo-dyes to limit their impacts on human health and ecosystems. Therefore, as possible future perspectives, the studied process can be considered as a proof of concept for an efficient azo-dyes treatment aimed to achieve both high degradation efficiency and reduced ecological impacts, making the treated effluent environmental friendly.

CRediT authorship contribution statement

Alice Cardito: Data curation, Formal analysis, Investigation, Writing - original draft. **Maurizio Carotenuto:** Conceptualization, Formal analysis, Validation, Writing - original draft. **Olga Sacco:** Investigation, Validation, Writing - original draft. **Luisa Albarano:** Data curation, Investigation, Writing - original draft. **Vincenzo Vaiano:** Methodology, Writing - original draft. **Patrizia Iannece:** Formal analysis, Investigation, Writing - original draft. **Giovanni Libralato:** Funding acquisition, Validation, Writing - review & editing. **Vincenzo Romano Spica:** Funding acquisition, Writing - review & editing. **Giusy Lofrano:** Conceptualization, Supervision, Validation, Writing - original draft, Writing - review & editing.

Declaration of competing interest

The authors declare that they have no known competing financial interests or personal relationships that could have appeared to influence the work reported in this paper.

Data availability

Data will be made available on request.

Appendix A. Supplementary data

Supplementary data to this article can be found online at https://doi.org/10.1016/j.envpol.2023.123226.

References

Albarano, L., Serafini, S., Toscanesi, M., Trifuoggi, M., Zupo, V., Costantini, M., Vignati, D.A.L., Guida, M., Libralato, G., 2022a. Genotoxicity set up in *Artemia franciscana* nauplii and adults exposed to phenanthrene, naphthalene, fluoranthene, and Benzo(k)fluoranthene. Water 14, 1594.

Albarano, L., Toscanesi, M., Trifuoggi, M., Guida, M., Lofrano, G., Libralato, G., 2022b. In situ microcosm remediation of polyaromatic hydrocarbons: influence and effectiveness of Nano-Zero Valent Iron and activated carbon. Environ. Sci. Pollut. Control Ser. 30, 3235–3251.

APAT, IRSA-CNR, 2003. Manuali e Linee Guida-Metodi Analitici per le Acque. Manuali e Linee Guida 29/2003 3, 1043–1049.

Banat, I.M., Nigam, P., Singh, D., Marchant, R., 1996. Microbial decolorization of textile-dye-containing effluents: a review. Bioresour. Technol. 58, 217–227.

Bandara, J., Mielczarski, J.A., Kiwi, J., 1999. Molecular mechanism of surface recognition. Azo dyes degradation on Fe, Ti, and Al oxides through metal sulfonate complexes. Langmuir 15, 7670–7679.

Bauer, C., Jacques, P., Kalt, A., 2001. Photooxidation of an azo dye induced by visible light incident on the surface of TiO_2. J. Photochem. Photobiol. Chem. 140, 87–92.

Cao, J., Wei, L., Huang, Q., Wang, L., Han, S., 1999. Reducing degradation of azo dye by zero-valent iron in aqueous solution. Chemosphere 38, 565–571.

El-Nemr, M.A., Abdelmonem, N.M., Ismail, I.M.A., Ragab, S., El Nemr, A., 2020. The efficient removal of the hazardous azo dye Acid Orange 7 from water using modified biochar from Pea-peels. Desalination Water Treat. 203, 327–355.

Fan, J., Guo, Y., Wang, J., Fan, M., 2009. Rapid decolorization of azo dye methyl orange in aqueous solution by nanoscale zerovalent iron particles. J. Hazard Mater. 166, 904–910.

Freyria, F.S., Bonelli, B., Sethi, R., Armandi, M., Belluso, E., Garrone, E., 2011. Reactions of acid orange 7 with iron nanoparticles in aqueous solutions. J. Phys. Chem. C 115, 24143–24152.

Freyria, F.S., Esposito, S., Armandi, M., Deorsola, F., Garrone, E., Bonelli, B., 2017. Role of pH in the aqueous phase reactivity of zerovalent iron nanoparticles with acid orange 7, a model molecule of azo dyes. J. Nanomater. 2017, 2749575.

Guan, J., Long, Z., Li, Q., Han, J., Du, H., Wang, P., Zhang, G., 2021. Citric acid modulated preparation of CdS photocatalyst for efficient removal of Cr(VI) and methyl orange. Opt. Mater. 121, 111604.

Libralato, G., 2014. The case of *Artemia* spp. in nanoecotoxicology. Mar. Environ. Res. 101, 38–43.

Lichtfouse, E., Schwarzbauer, J., Robert, D., Dir, 2015. Pollutants in buildings, water and living organisms. Eric Lichtfouse, jan Schwarzbauer, Didier Robert. Springer Nature 7, 348.

Lim, C.K., Bay, H.H., Neoh, C.H., Aris, A., Abdul Majid, Z., Ibrahim, Z., 2013. Application of zeolite-activated carbon macrocomposite for the adsorption of Acid Orange 7: isotherm, kinetic and thermodynamic studies. Environ. Sci. Pollut. Control Ser. 20, 7243–7255.

Lofrano, G., Libralato, G., Adinolfi, R., Siciliano, A., Iannece, P., Guida, M., Giugni, M., Volpi Ghirardini, A., Carotenuto, M., 2016. Photocatalytic degradation of the antibiotic chloramphenicol and effluent toxicity effects. Ecotoxicol. Environ. Saf. 123, 65–71.

Mielczarski, J.A., Montes Atenas, G., Mielczarski, E., 2005. Role of iron surface oxidation layers in decomposition of azo-dye water pollutants in weak acidic solutions. Appl. Catal. B Environ. 56, 289–303.

Nam, S., Tratnyek, P.G., 2000. Reduction of azo dyes with zero-valent iron. Water Res. 34, 1837–1845.

Nunes, B.S., Carvalho, F.D., Guilhermino, L.M., Van Stappen, G., 2006. Use of the genus *Artemia* in ecotoxicity testing. Environ. Pollut. 144, 453–462.

Perera, H.J., 2019. Removal of acid orange 7 dye from wastewater: review. Int. J. Wine Res. 9, 1000367.

Perez-Calderon, J., Marin-Silva, D.A., Zaritzky, N., Pinotti, A., 2023. Eco-friendly PVA-chitosan adsorbent films for the removal of azo dye Acid Orange 7: physical cross-linking, adsorption process, and reuse of the material. Adv. Ind. Eng. Polym. Res. 6, 239–254.

Rathi, B.S., Kumar, P.S., 2021. Application of adsorption process for effective removal of emerging contaminants from water and wastewater. Environ. Pollut. 280, 116995.
Rauf, M.A., Meetani, M.A., Hisaindee, S., 2011. An overview on the photocatalytic degradation of azo dyes in the presence of TiO_2 doped with selective transition metals. Desalination 276, 13–27.
Rescigno, R., Sacco, O., Pragliola, S., Albarano, L., Libralato, G., Lofrano, G., et al., 2023. Environmentally safe ZVI/ZnS-based polymer composite for lindane degradation in water: assessment of photocatalytic activity and eco-toxicity. Separ. Purif. Technol. 330, 125246.
Roy, G., de Donato, P., Görner, T., Barres, O., 2003. Study of tropaeolin degradation by iron—proposition of a reaction mechanism. Water Res. 37, 4954–4964.
Sacco, O., Vaiano, V., Navarra, W., Daniel, C., Pragliola, S., Venditto, V., 2021. Catalytic system based on recyclable Fe^0 and ZnS semiconductor for UV-promoted degradation of chlorinated organic compounds. Separ. Purif. Technol. 270, 118830.
Satapanajaru, T., Chompuchan, C., Suntornchot, P., Pengthamkeerati, P., 2011. Enhancing decolorization of Reactive Black 5 and Reactive Red 198 during nano zerovalent iron treatment. Desalination 266, 218–230.
Sivakumar, D., 2014. Role of Lemna minor Lin in treating the textile industry wastewater. Int. J. Environ. Ecol. Geol. Min. Eng. 8, 203–220.
Sonwani, R.K., Pandey, S., Yadav, S.K., Giri, B.S., Katiyar, V., Singh, R.S., Rai, B.N., 2021. Construction of integrated system for the treatment of Acid orange 7 dye from wastewater: optimization and growth kinetic study. Bioresour. Technol. 337, 125478.
Xiong, H., Zhang, B., Cui, C., Xu, Y., 2022. Polyaniline/FeOOH composite for removal of Acid Orange II from aqueous solutions. Mater. Chem. Phys. 278, 125701.
Yaseen, D.A., Scholz, M., 2019. Textile dye wastewater characteristics and constituents of synthetic effluents: a critical review. Int. J. Environ. Sci. Technol. 16, 1193–1226.
Zhang, F., Yediler, A., Liang, X., Kettrup, A., 2004. Effects of dye additives on the ozonation process and oxidation by-products: a comparative study using hydrolyzed CI Reactive Red 120. Dyes Pigments 60 (1), 1–7.
Zhang, C., Zhu, Z., Zhang, H., Hu, Z., 2012. Rapid decolorization of Acid Orange II aqueous solution by amorphous zero-valent iron. J. Environ. Sci. 24, 1021–1026.
Zhao, Z., Cao, Y., Li, S., Zhang, Y., 2021. Effects of biowaste-derived biochar on the electron transport efficiency during anaerobic acid orange 7 removal. Bioresour. Technol. 320, 124295.
Zhong, X., Xiang, L., Royer, S., Valange, S., Barrault, J., Zhang, H., 2011. Degradation of C.I. Acid Orange 7 by heterogeneous Fenton oxidation in combination with ultrasonic irradiation. J. Chem. Technol. Biotechnol. 86, 970–977.
Zhu, K., Wang, X., Chen, D., Ren, W., Lin, H., Zhang, H., 2019. Wood-based biochar as an excellent activator of peroxydisulfate for Acid Orange 7 decolorization. Chemosphere 231, 32–40.